The Effects of Freestream Turbulence on Wing-Gust Interactions

Colin M. Stutz*
NASA Langley Research Center, Hampton, VA, 23681, USA

John T. Hrynuk†
DEVCOM Army Research Lab, Aberdeen Proving Ground, MD, 21005, USA

Douglas G. Bohl‡
Clarkson University, Potsdam, NY, 13699, USA

There is a growing interest in the experimental study of discrete vertical gusts motivated by the proliferation of small Uncrewed Air Systems. However, gusts are not the only unsteady flow disturbances that these vehicles are expected to encounter. Freestream turbulence is also a serious consideration. Previous work has indicated that freestream turbulence has significant effects on the flow around airfoils, so this work investigates the interaction of these two unsteady flow disturbances. Airfoils are pitched to mimic the flow angle change caused by a gust at different levels of incoming freestream turbulence. The lift generated during the gust encounters with elevated incoming freestream turbulence show that the effects on the performance of the airfoil are dependent on the turbulence intensity. Low turbulence intensity has beneficial effects, delaying stall and increasing the maximum lift, whereas higher freestream turbulence intensity delays stall without a corresponding increase in the maximum lift. A preliminary investigation of 15-trial ensemble-averaged flow fields suggests that freestream turbulence dominates the flow, but the flow features associated with the dynamic lift seen in the "clean" case are still somewhat present. However, lift curves and flow fields from individual trials indicate that the turbulence increases the unsteadiness in the interaction, but the general trends are dominated by the gust interaction. Further work is still needed to better determine the flow physics of these interactions and the interplay between repeatable and stochastic flow phenomena.

I. Nomenclature

α	=	angle of attack, degrees
c	=	chord, meters
C_L	=	coefficient of lift
$FSTI$	=	Freestream Turbulence Intensity, (U_{rms}/U_{mean})x100%
GR	=	gust ratio, $GR = v/U_\infty$
L_x	=	Turbulent length scale, meters
ω	=	Vorticity, 1/s
rms	=	root mean square subscript
t	=	time, seconds
t^*	=	convective time, $t^* = U_\infty t/c$
U_∞	=	freestream velocity, meters per second
u	=	velocity component in x direction, meters per second
v	=	velocity component in y direction, meters per second

II. Introduction

The growing popularity of small Uncrewed Air Systems (sUAS) has led to an increased interest in studying the flow regimes that such vehicles inhabit. The small size and weight of these vehicles, coupled with their low speeds, make

*Aerospace Research Engineer, Aeroacoustics Branch, 2 N. Dryden Street, AIAA Member.
†Research Mechanical Engineer, Army Research Directorate, 6340 Rodman Road, AIAA Member.
‡Professor, Department of Mechanical and Aerospace Engineering, 8 Clarkson Ave. Box 5725.

them especially susceptible to unsteady flow disturbances [1]. One such disturbance that many sUAS are anticipated to encounter, especially in urban environments, is vertical gusts, and as such there is an expanding interest in studying these discrete vertical gust encounters. Vertical gusts are defined as an introduction of a vertical velocity component to otherwise horizontal flight, and their strength is characterized by gust ratio, where $GR = v/U_\infty = \tan(\alpha_{flow})$ [2]. Mohamed et al. [3] and White et al. [4] investigated the flow past a building numerically and experimentally, respectively, and found that gusts could be as strong as GR = 1, i.e., flow angles as high as 45°. Even gust ratios as low as GR = 0.2 (α_{flow} = 11.3°) could lead to flow angles above the static stall angle for many airfoils at lower Reynolds numbers [5]. Some gusts have also been observed to develop at high enough rates to generate transient dynamic lift [5] or large, repeatable leading-edge vortices [6, 7]. These factors highlight the importance of continuing research on gust interactions at scales that are relevant to sUAS.

Small UAS typically fly at lower altitudes than traditional crewed aircraft. These lower altitudes mean that sUAS must deal with the unsteadiness inherent in the atmospheric boundary layer, specifically freestream turbulence [8]. Watkins et al. [8] investigated this low-altitude turbulence with a rake of probes placed on a stand on the roof of a vehicle driving at a variety of speeds in multiple surroundings. The resulting data indicated that freestream turbulence intensity (FSTI = u_{rms}/u_{mean}x100%) experienced an exponential decay as the freestream speed of the vehicle increased, with FSTI < 5% at speeds above 30 m/s but as high as 30% at 5 m/s. This suggests that the presence of freestream turbulence is a factor that must be considered for sUAS flight. Olson [9] investigated the effects of freestream turbulence on the boundary layer of an SD7003 airfoil at low Reynolds numbers ($O(10^4)$). The "baseline" cases (FSTI < 0.5%) showed large reverse regions beneath separated boundary layers at higher angles of attack. However, the addition of freestream turbulence (FSTI ≈ 1.5%) led to the boundary layers staying almost completely attached along the entire chord of the airfoil. This suggests that the addition of even a small amount of freestream turbulence has the potential to completely change the flow physics for a static airfoil at low Reynolds numbers. Recent work at DEVCOM ARL on the effects of freestream turbulence on the static lift curves of airfoils at low Reynolds numbers also demonstrated that the presence of freestream turbulence significantly changes the performance of the airfoils [10, 11]. When taken together, these results indicate that sUAS *will* encounter freestream turbulence during regular operation, and its presence will likely alter the flow and performance characteristics of the lifting surfaces. This is an especially important factor to consider given that, historically, great efforts have been made to ensure the lowest possible amounts of freestream turbulence in experimental environments.

This work will investigate the interaction of two unsteady flow disturbances: freestream turbulence and discrete vertical gust interactions. One goal of the current study is to determine if one disturbance is clearly dominant. Conversely, if the disturbances interact, does the interaction take the form of a type of superposition that can be readily understood and even predicted? Preliminary results include combined flow fields from repeated trials and pressure-derived lift histories from the gust encounters.

III. Experimental Methods

The experiments in this work were conducted in the Microsystems Aeromechanics Wind Tunnel at the DEVCOM Army Research Laboratory (ARL). This tunnel has a test section with a cross-sectional area of 0.91 m x 0.91 m (3 ft x 3 ft) and a length of 1.83 m (6 ft) and is capable of speeds between 1 and 100 m/s. Two airfoil models were used, with NACA 0012 and Eppler 387 cross sections, 12 cm chords, and 50.8 cm spans. The models were mounted between false walls in the center of the test section and connected on one side to a servomotor at 1/4-chord. Pitching motions, which will be described in detail later, were controlled by a 4,000 count per revolution (angular resolution of ≈ 0.1°) servomotor operated by a Galil 4020 servo controller [12]. Flow field data were collected at the model midspan using high-speed Particle Image Velocimetry (PIV). The PIV data were collected at 100 Hz with LaVision's DaVis 10 software. Two Phantom v641 cameras and a Photonics Model DM 100 dual-cavity laser were used in conjunction with a mirror system that directed a portion of the laser sheet underneath the model. This allowed for the collection of time-resolved, instantaneous, full-field flow data to be collected. Fifteen repeated trials were combined and fit to a regular grid using the method described by Cohn and Koochesfahani [13]. Vorticity was then calculated using the regularly spaced velocity fields. Uncertainty for the combined flow fields was determined to be below 3% using the methods described and validated by Wieneke [14].

This work will focus on an existing, well characterized, experimentally generated prolonged gust: the GR 0.3 gust at Re = 12x10^3 from Stutz et al. [5]. The original gust was generated by an aerodynamic blockage via a vertical jet from the floor of the test section. Stutz et al. [5] observed that the jet bent in the direction of the freestream flow, creating a blockage that the freestream flow then deflected over, which introduced the vertical velocity component of the gust. Lift

was then directly measured during the gust encounter with NACA 0012, Eppler 387, and SD 5060 airfoils. All three airfoils experienced a rapid increase in lift, along with a period of dynamic lift that was above the steady-gust lift, before settling at a steady-gust lift condition. The lift profiles during the gust interactions were observed by Stutz et al. [5] to stabilize to steady lift values, when the gust was fully developed, which were similar to the expected C_L from the static lift curves at the same angle as the maximum flow angle of the gust. This is called the "steady-gust" condition. The onset of the dynamic lift was observed in the flow fields to be caused by a delay in the development of the flow near the upper surface of the airfoil. Most drastically, this presented as a reattachment of the boundary layer near the trailing edge of the NACA 0012. Stutz [15] demonstrated that the major flow structures of the gusts in Stutz et al. [5] could be successfully replicated with a two-slope linear pitching motion of the airfoil in steady flow. The flow in the pure-pitching gust replication cases was observed to have more distinct vortical structures, likely due to the increased repeatability between trials of the pitching motion compared to the generated gust. It was determined that removing the variability between repeated trials in the gust would be beneficial for this study, leaving the freestream turbulence to be the only component with obvious run-to-run variability. The GR 0.3 gust was replicated using a pitching motion that was an exact match of the flow angle characterization from Stutz et al. [5], which is shown in Fig. 1. This pitching motion was performed with NACA 0012 and Eppler 387 airfoils to replicate the GR 0.3 gust at the same chord-based Reynolds number of $12\text{x}10^3$ as the original work.

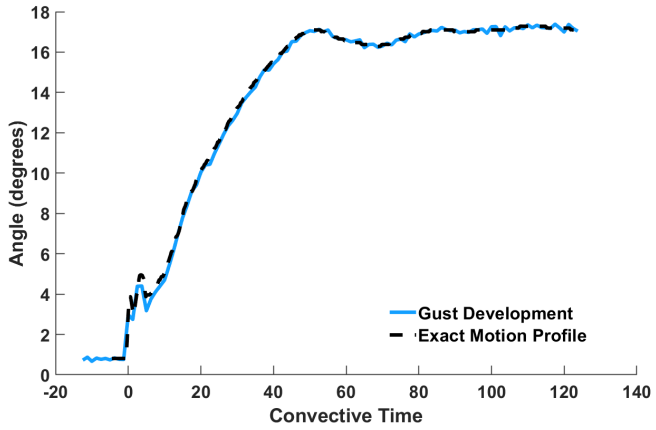

Fig. 1 Comparison of the Flow Angle Characterization from Stutz et al. [5] and the Pure-Pitching Approximation Motion for the GR 0.3 Gust.

Accurate direct force measurement in air is difficult at the Reynolds number investigated in this work (U_∞ = 1.5 m/s, Re = $12\text{x}10^3$). The low speed and low dynamic pressure lead to very small aerodynamic forces, and the rapid pitching motions make the aerodynamic forces difficult to properly isolate. As such, a method has been developed to calculate the aerodynamic forces from the flow fields. This was done by determining the pressure fields using the PIV data, extracting the surface pressure, and then integrating to calculate lift. The pressure fields were determined by first calculating the pressure gradient field, ∇P, which can be done using the velocity fields. The pressure gradient field was then broken up into the following regions based on the expected complexity of the flow, from simplest to most complex: outer region, wake region, near-edge region (circles centered at the leading and trailing edges), and the near-body region [16]. A simple spatial-marching routine [17], constrained by a field-erosion principle, which requires a minimum number of known points as inputs [18], was then used to integrate the regions in order from least complex to most complex. An isentropic flow relationship [18] was used as a boundary condition in an upstream corner of the field of view for the outer region. Each solved region was then used as the boundary condition for the next-most-complex region. The pressure was then extracted from near the airfoil surface to determine the lift [19].

The freestream turbulence was generated by passive grids placed between the end of the contraction and the start of the test section. This placed the models 4 chord lengths downstream of the turbulence grids. Three cases were investigated: a "clean" flow case, where no grid was in place, and two grids referred to as the Low Turbulence Generator (LTG) and High Turbulence Generator (HTG). The grids were constructed of cylindrical wooden dowels in a Cartesian grid pattern. Dimensions and basic turbulence characteristics for the three cases are given in Table 1. The grid spacings for the LTG and HTG grids were selected to maintain a nominal open area of 65%. Freestream velocity, freestream turbulence intensity, and turbulent length scale (L_x) were measured using a single-axis hot-wire probe placed in the test

section at the same location as the center of the test models. Small discrepancies in the freestream speed due to the blockages inherent in the passive turbulence grids were accounted for when determining normalized lift coefficients.

Table 1 Turbulence Generator Dimensions

Turbulence Case	Wire Diameter	Spacing	U_{mean} (m/s)	U_{rms} (m/s)	FSTI (%)	L_x (cm)
"Clean" Baseline	-	-	1.509	0.0083	0.52	0.003
LTG	0.953 cm (0.375 in)	2.86 cm (1.125 in)	1.568	0.0397	2.53	1.435
HTG	3.18 cm (1.25 in)	9.53 cm (3.75 in)	1.574	0.1098	6.97	2.646

IV. Results and Discussion

The force histories from the three cases for both airfoils were calculated using the method described in Section III. The force histories are then given in Fig. 2. A light smoothing was applied to the pressure-derived lift curves to allow for easier visual comparison using a 15-point moving mean filter. The "clean" flow cases for both airfoils demonstrate the dynamic lift observed in Stutz et al. [5], seen from $15 \lesssim t^* \lesssim 40$. This dynamic lift region can be defined as when the airfoil generated lift above the static maximum in a transient fashion. After the dynamic lift event, the lift then settled to a steady-gust condition ($t^* \gtrsim 40$) for the NACA 0012 and a cyclical vortex-shedding-induced steady-gust condition for the Eppler 387. The airfoils still experienced dynamic lift for the LTG and HTG cases, with a period of lift higher than the steady-gust lift. For both airfoils, a small amount of turbulence (FSTI = 2.5%) generally did not affect the lift production until the dynamic lift region. Both airfoils experienced a higher peak C_L at a later time for the LTG case. The shape of the lift curves for the LTG cases suggest that the early portion of the dynamic lift period was similar to the baseline "clean" case, but the presence of freestream turbulence extended the dynamic lift event for a longer time than in the "clean" flow. However, when the freestream turbulence was increased, the change in the lift data was more dramatic. The slope of the lift curve decreased, with roughly the same peak lift as the "clean" flow case but occurring later in time. The divergence in the turbulent lift curves from the "clean" flow case occurred at the same time as when the "clean" case began to experience the dynamic lift, $t^* \approx 15$.

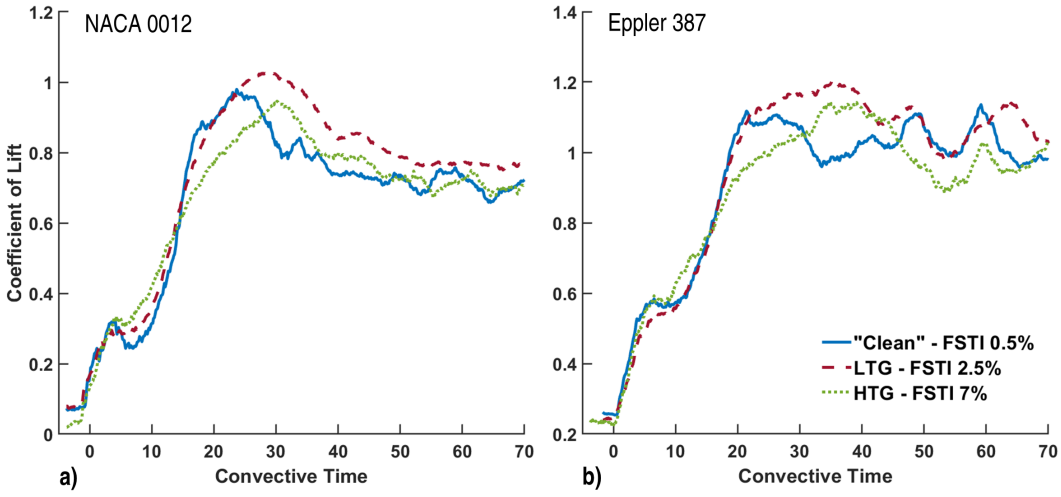

Fig. 2 Effects of Freestream Turbulence on GR 0.3 Wing-Gust Interaction Lift Profile for (a) NACA 0012 and (b) Eppler 387.

The effects of freestream turbulence on the lift generated during a wing-gust interaction are difficult to interpret alone, but the flow fields may help in understanding the flow physics. Figure 3 shows flow fields for the NACA 0012 at

three points during the gust interaction, which are marked on the lift curves. First is the point at which the lift first exceeds the steady-gust lift, which represents the beginning of the dynamic lift region. Next is the point of peak lift for each case, and the last point is roughly where the lift reaches the fully developed gust condition. The original experimental study of this gust, Stutz et al. [5], found that the boundary layer had started to separate as the flow angle increased and reattached at the trailing edge during the period of dynamic lift. The boundary layer then re-separated as the lift returned to the fully developed gust condition. This series of events was successfully recreated by the "clean" flow case, which is shown in the left column of Fig. 3. The presence of freestream turbulence, center and right columns of Fig. 3, appeared to drastically change the behavior of the flow during the gust interaction. As reported by Olson [9] for static airfoils, the presence of freestream turbulence in the flow leads to the boundary layer being attached along the entire chord of the airfoil, well past the static stall angle (≈8° for a NACA 0012 at Re = $12x10^3$). Although there was not a clear separation and reattachment for the turbulence cases, the streamlines for both indicate that near the point of peak lift, the flow remained attached at the trailing edge. The effect is more easily observed for the lower turbulence case at peak lift, where the streamlines bend toward a reattachment point well past the static stall angle of this airfoil at this Reynolds number (α = 8°). This suggests that although the freestream turbulence changed some features of the flow and lift generation, the gust and turbulence effects contributed in such a way that neither one dominated the overall flow behavior. All three cases showed similar fully separated flows, corresponding to the force profiles reaching the steady-gust lift condition.

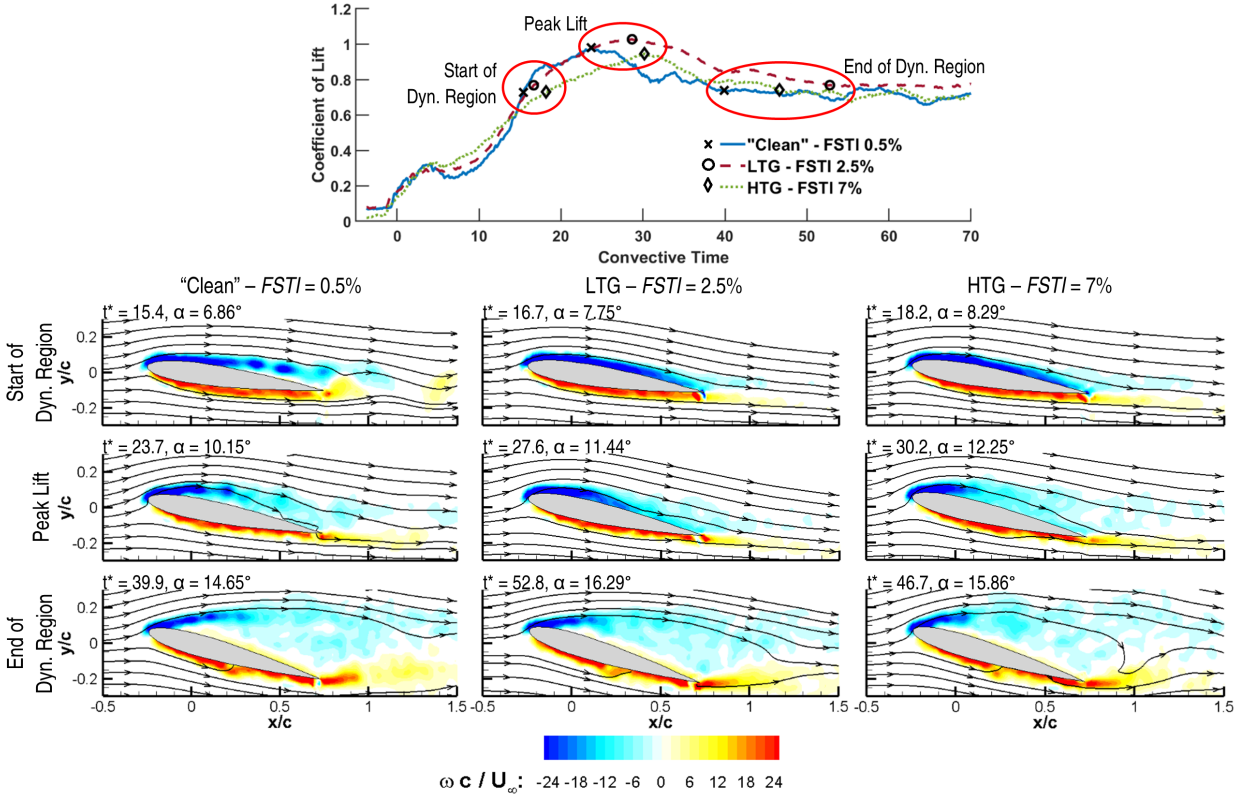

Fig. 3 Effects of Freestream Turbulence on GR 0.3 Wing-Gust Interaction Flow Physics for NACA 0012 at Important Times - Visualized as Normalized Vorticity.

Stutz et al. [5] demonstrated that the separation and reattachment of the boundary layer was more readily observable in contours of u-velocity as opposed to vorticity. Figure 3 was reproduced highlighting u-velocity in Fig. 4 to show reverse flow regions. The separation at the trailing edge and the reattachment corresponding with peak lift for the "clean" case are more easily observed in Fig. 4, with reverse flow (blue) along the airfoil surface indicating separation. Similarly, it is clear that the flow was completely attached until very high angle for the LTG and HTG cases.

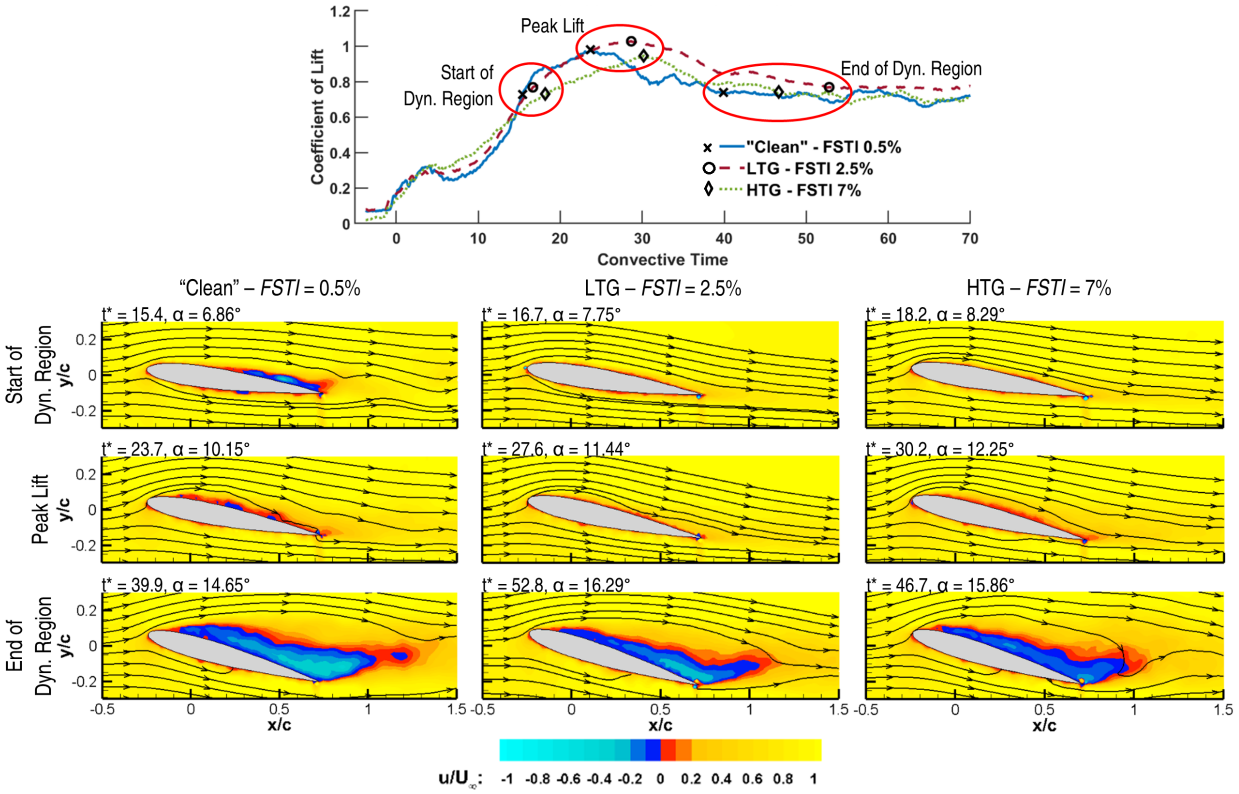

Fig. 4 Effects of Freestream Turbulence on GR 0.3 Wing-Gust Interaction Flow Physics for NACA 0012 at Important Times - Visualized as Normalized *u*-Velocity.

Figures 3 and 4 also demonstrate an interesting, but not new, challenge when investigating freestream turbulence. High-speed PIV and highly repeatable pitching motions couple with a stochastic flow phenomenon like freestream turbulence in such a way that may make the standard method of combining repeated trials unrepresentative of the actual flow. In essence, the combined flow fields from 15 repeated trials shown here act as a time-resolved averaged flow, where individual turbulent structures, which are nonrepeatable, are averaged out. In these averages of repeated trials, the gust generation is highly repeatable, but the exact mechanisms of how the turbulence interacts with the repeatable flow structures may not be adequately captured.

The first five repeated trials for the LTG and HTG cases for the NACA 0012 were individually processed as a first step in investigating the interaction of repeatable and stochastic flow phenomena. These single-run cases were expected to be significantly more sensitive to any noise in the data. Figure 5 shows the pressure-derived lift from these individual repeated trails compared with the derived lift from the 15-trial ensemble, which was given in Fig. 2(a). Figures 5(a) and (b) demonstrate the highly unsteady nature of the freestream turbulence by comparing the raw lift curves to the ensemble-averaged data, where the cyan curve is the raw ensemble-averaged data and the black curve has the same 15-point moving mean filter as was used on the curves in Fig. 2. The moving mean filter is then applied to the lift curves from the individual trials and compared to the ensemble-averaged curves in Figs. 5(c) and (d). These results show that the individual trials and the ensemble-averaged data follow the same trends, which are similar to the gust interaction in a nominally clean freestream. This suggests that the overall trend in lift during the gust interaction is not affected by the presence of freestream turbulence. However, there may be large deviations at any point in time between an individual interaction and the mean.

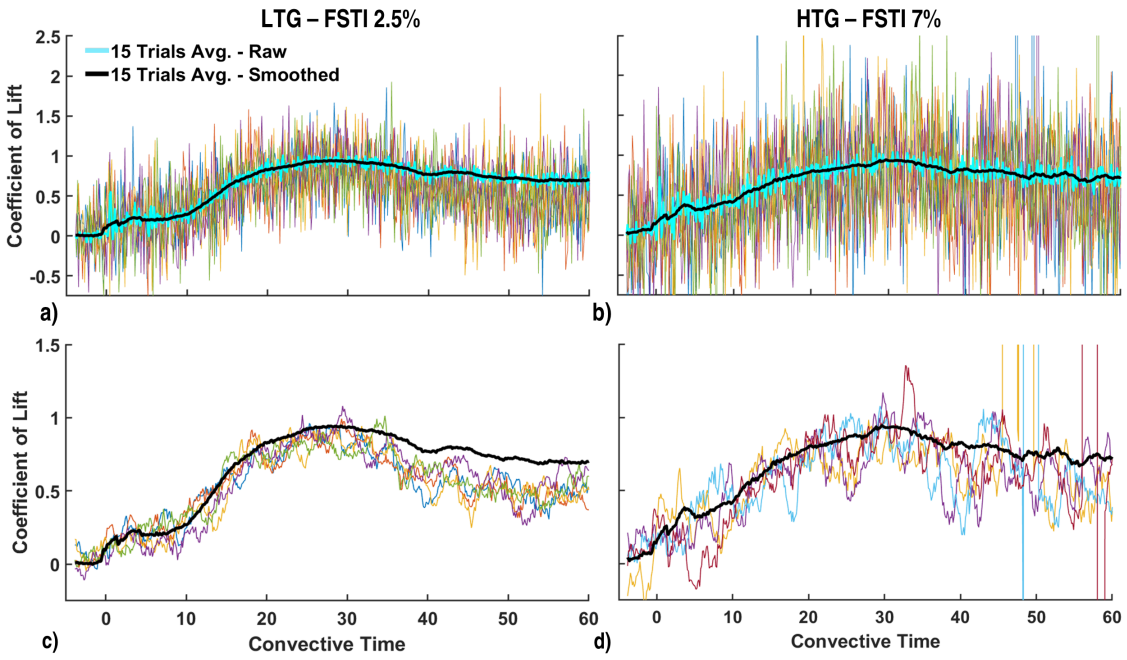

Fig. 5 Raw (top) and lightly smoothed (bottom) lift curves for the first five repeated trails (colored lines) and the combined 15-trial dataset for the NACA 0012.

A subset of flow fields is shown in Figure 6 for the three points in the interaction identified in Fig. 4. The interaction that occurred in "clean" flow shows clear vortical shedding from the upper surface at the start of the dynamic lift region (first column). The ensemble-averaged flow field for the HTG case for the same period indicates completely attached flow. However, although it is difficult to tell with still images, the flow fields from the individual trials also exhibit vortex shedding from the upper surface. For these cases, vortices were observed to begin forming in the boundary layer near the quarter-chord location. Instead of separating from the surface and shedding, the vortices convected along the airfoil surface and only leave the surface near the trailing edge. Initial observations suggest that passing turbulent structures in the flow may be preventing the detachment of the vortices from the boundary layer. This stochastic behavior is also seen in the flow fields at the point of peak lift, where the streamlines in the "clean" flow case clearly show a reattachment of the boundary layer to the airfoil at the trailing edge. The ensemble-averaged flow field also appears to show that the boundary layer trends toward the surface at the trailing edge on average. However, similar to the start of the dynamic region, the path of the shedding boundary layer in the individual trials is disturbed by the freestream turbulence. HTG Trial 1 (Fig. 6, third row) shows a very similar flow field to the "clean" flow average. However, HTG Trial 2 (Fig. 6, fourth row) appears to show a completely attached boundary layer. A shedding vortical structure observed in HTG Trial 3 seems to split the difference between the other two cases. Based on these results, along with the lift data, it appears that the effects of turbulence reattaching the boundary layer [11] mix with the dynamic lift generation observed for gusts in Stutz et al. [5].

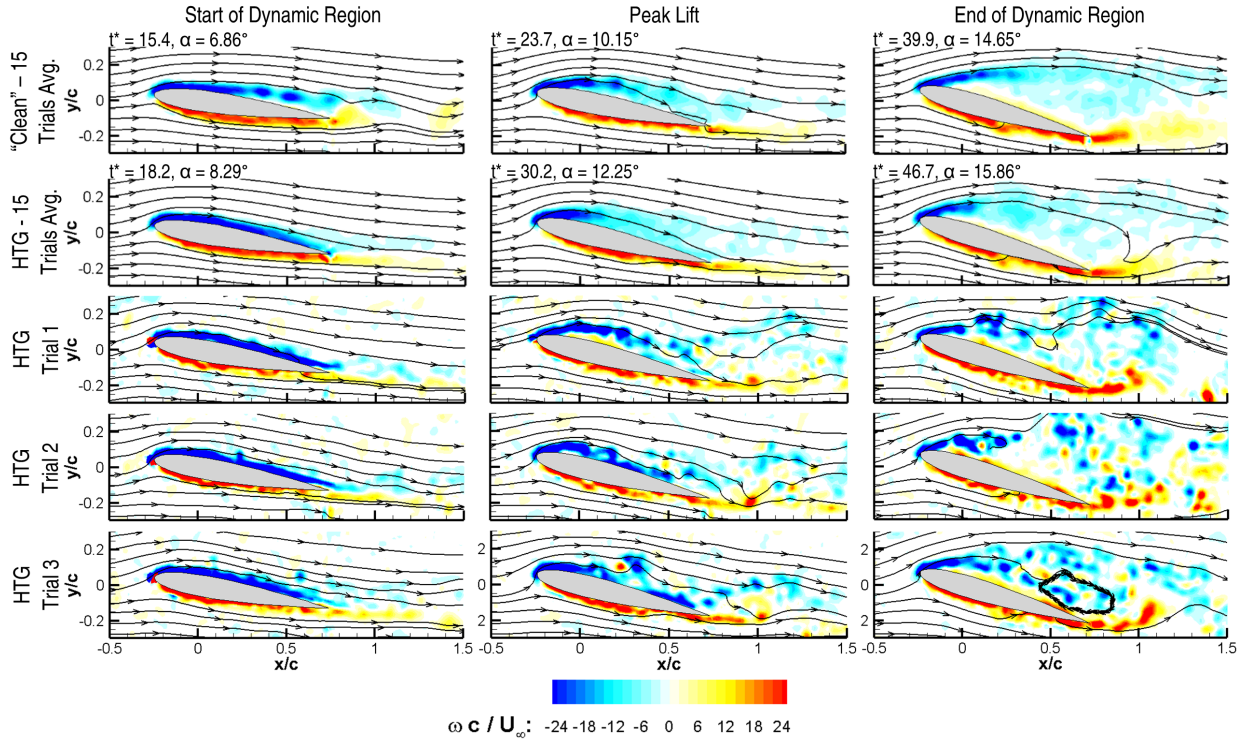

Fig. 6 A comparison of the flow fields for the "Clean" and HTG cases from Figure 4 with a subset of the individual trials. Note that all HTG cases in the same column occur at the same *t and angle.**

V. Conclusions

This work investigates the interplay between two unsteady flow disturbances, discrete vertical gusts and freestream turbulence. Two airfoils were pitched to simulate an interaction with the GR 0.3 gust from Stutz et al. [5] in three different amounts of freestream turbulence. Preliminary results show that lower levels of freestream turbulence (2.5% FSTI) slightly increase the maximum dynamic lift experienced during the interaction and delay the stall point compared to "clean" flow (0.5% FSTI). However, a larger amount of freestream turbulence (7% FSTI) delays the stall point but has a negligible or detrimental effect on the maximum generated lift. Investigation of the ensemble-averaged flow fields for the NACA 0012 shows that, unlike in "clean" flow, there was no initial separation and reattachment of the boundary layer associated with the dynamic lift. Instead, the boundary layer stayed generally attached to the upper surface of the airfoil for the turbulence cases, with higher turbulence generating a significantly larger boundary layer. Streamlines indicated that the flow continued to bend and reattach for all cases, but with turbulence causing some variability in this process.

A subset of repeated trials for the NACA 0012 in 7% FSTI (the HTG case) were analyzed to investigate the interplay between the highly repeatable simulated gust interaction and the stochastic freestream turbulence. Pressure-derived lift curves from these cases suggest that the overall trends in lift generation are dominated by the gust interaction, but the freestream turbulence greatly increases the unsteadiness in the lift. The flow field data from these trials supported the assertion that the standard ensemble-averaging method utilized when studying many repeatable flow phenomena likely captures the trends in the flow on average but misses the stochastic processes in an individual interaction. The results show a complex mixing of turbulence effects with the dynamic lift generation observed for gusts. More work must be done to understand how the dynamic lift in gust events is generated and how turbulence alters those flow mechanics.

Future work will include extending the investigation of the flow fields to the Eppler 387 airfoil, specifically to confirm that the observed flow physics are not airfoil dependent. More work will also be done to interrogate the interplay between the two unsteady flow phenomena. Of specific interest is if the effects of freestream turbulence on repeatable unsteady flows can be captured by accounting for the effects on the static performance of the airfoil, which is easy to measure. Also, there is likely value in determining if the classic ensemble-averaging method is viable for studying problems like these if the only consideration is on-average broad trends, and the run-to-run stochastic variation is of less concern.

Acknowledgments

Research was sponsored by the Army Research Laboratory and was accomplished under Cooperative Agreement Number W911NF-19-2-0197. The views and conclusions contained in this document are those of the authors and should not be interpreted as representing the official policies, either expressed or implied, of the Army Research Laboratory or the U.S. Government. The U.S. Government is authorized to reproduce and distribute reprints for Government purposes notwithstanding any copyright notation herein.

References

[1] Richardson, J. R., Atkins, E. M., Kabamba, P. T., and Girard, A. R., "Scaling of Airplane Dynamic Response to Stochastic Gusts," *Journal of Aircraft*, Vol. 51, No. 5, 2014, pp. 1554–1566. https://doi.org/10.2514/1.C032410.

[2] Stutz, C. M., Hrynuk, J. T., and Bohl, D. G., "Dimensional Analysis of a Transverse Gust Encounter," *Aerospace Science and Technology*, Vol. 137, 2023. https://doi.org/10.1016/j.ast.2023.108285.

[3] Mohamed, A., Watkins, S., Ol, M. V., and Jones, A. R., "Flight-Relevant Gusts: Computation-Derived Guidelines for Micro Air Vehicle Ground Test Unsteady Aerodynamics," *Journal of Aircraft*, Vol. 58, No. 3, 2021, pp. 693–699. https://doi.org/10.2514/1.C035920.

[4] White, C., Lim, E., Watkins, S., Mohamed, A., and Thompson, M., "A feasibility study of micro air vehicles soaring tall buildings," *Journal of Wind Engineering and Industrial Aerodynamics*, Vol. 103, 2012, pp. 41–49. https://doi.org/10.1016/j.jweia.2012.02.012.

[5] Stutz, C. M., Hrynuk, J. T., and Bohl, D. G., "Investigation of static wings interacting with vertical gusts of indefinite length at low Reynolds numbers," *Experiments in Fluids*, Vol. 63, 2022, p. 82. https://doi.org/10.1007/s00348-022-03432-7.

[6] Corkery, S., Babinsky, H., and Harvey, J., "On the development and early observations from a towing tank-based transverse wing-gust encounter test rig," *Experiments in Fluids*, Vol. 59, 2018, p. 135. https://doi.org/10.1007/s00348-018-2586-0.

[7] Sedky, G., Jones, A. R., and Lagor, F. D., "Lift Regulation During Transverse Gust Encounters Using a Modified Goman-Khrabrov Model," *AIAA Journal*, Vol. 58, No. 9, 2020, pp. 3788–3798. https://doi.org/10.2514/1.J059127.

[8] Watkins, S., Milbank, J., Loxton, B. J., and Melbourne, W. H., "Atmospheric Winds and Their Implications for Microair Vehicles," *AIAA Journal*, Vol. 44, No. 11, 2006, pp. 2591–2600. https://doi.org/10.2514/1.22670.

[9] Olson, D. A., "Facility and Flow Dependency Issues Influencing the Experimental Characterization of a Laminar Separation Bubble at Low Reynolds Number," Master's thesis, Michigan State University, 2011.

[10] Mackie, M., Stutz, C., and Hrynuk, J., "Examining the Effects of Turbulence on Low-Speed Airfoil Lift Performance," *75th Annual Mtg. of the Divison of Fluid Dynamics*, Indianapolis, Indiana, 2022.

[11] Hrynuk, J. T., Olson, D., Stutz, C., and Jackson, J., "Effects of Turbulence on NACA 0012 Airfoil Performance at Low Reynolds Number," *AIAA Journal*, 2023. https://doi.org/10.2514/1.J063244, URL https://doi.org/10.2514/1.J063244.

[12] Galil, *Galil Motion Controller DMC - 40X0 Datasheet*, Galil, 270 Technology Way, Rocklin, CA 95765 USA, 2020.

[13] Cohn, R. K., and Koochesfahani, M. M., "The accuracy of remapping irregularly spaced velocity data onto a regular grid and the computation of vorticity," *Experiments in Fluids*, Vol. 29, 2000, pp. S61–S69. https://doi.org/10.1007/S003480070008.

[14] Wieneke, B., "PIV uncertainty quantification from correlation statistics," *Measurement Science and Technology*, Vol. 26, 2015. https://doi.org/10.1088/0957-0233/26/7/074002.

[15] Stutz, C., "Experimental Study of Gust-Wing Interactions at Low Reynolds Numbers," Ph.D. thesis, Clarkson University, 2022.

[16] Jin Jeon, Y., Gomit, G., Earl, T., Chatellier, L., and David, L., "Sequential least-square reconstruction of instantaneous pressure field around a body from TR-PIV," *Experiments in Fluids*, Vol. 59, 2018, p. 27. https://doi.org/10.1007/s00348-018-2489-0.

[17] Baur, T., and Köngeter, J., "PIV with high temporal resolution for the determination of local pressure reductions from coherent turbulence phenomena," *3rd International Workshop on Particle Image Velocimetry*, University of California - Santa Barbara, 1999.

[18] van Oudheusden, B. W., "Principles and application of velocimetry-based planar pressure imaging in compressible flows with shock," *Experiments in Fluids*, Vol. 45, 2008, pp. 657–674. https://doi.org/10.1007/s00348-008-0546-9.

[19] Lucas, K. N., Dabiri, J. O., and Lauder, G. V., "A pressure-based force and torque prediction technique for the study of fish-like swimming," *PLoS ONE*, Vol. 12, 2017, p. 12. https://doi.org/10.1371/journal.pone.0189225.